Supporting Information

Self-assembly of Pt-based truncated octahedral crystals into metal-frameworks towards enhanced electrocatalytic activity

*Yunpeng Zuo[†a], Tingting Li[†a], Huan Ren[b], Guilin Zhu[a], Kai Han[a], Lin Zhuang[b] and Heyou Han[a]**

†These authors contributed equally to this work.
[a] State Key Laboratory of Agricultural Microbiology, College of Science, Huazhong Agricultural University, Wuhan 430070, P R China. E-mail: hyhan@mail.hzau.edu.cn.
[b] College of Chemistry and Molecular Sciences, Hubei Key Lab of Electrochemical Power Sources, Wuhan University, Wuhan 430072, P.R. China.

Materials: Pt/C (20% Pt) and oleic acid were purchased from Sigma-Aldrich. Chloroplatinic acid hexahydrate ($H_2PtCl_6 \cdot 6H_2O$, AR), N,N-Dimethylformamide (DMF, AR), Copper(Ⅱ) nitrate trihydrate, perchloric acid ($HClO_4$, 70%) were supplied by Sinopharm Chemical Reagent Co., Ltd. Unless special instructions, other chemicals were of analytical reagent. Ultrapure water for the whole experiment process was with a conductivity of 18.25 MΩ-cm.

Electrochemical Measurements.

The Koutecky-Levich equation as shown in equation (1) was used to analyze the kinetic currents of the ORR polarization curves and the ORR performance in the diffusion and kinetically limited regions normalized against the ECSA and Pt mass.

$$\frac{1}{j} = \frac{1}{j_k} + \frac{1}{j_d} \quad (1)$$

Where, j is the measured current density,

j_k is the kinetic current density,

j_d is the diffusion limited current density.

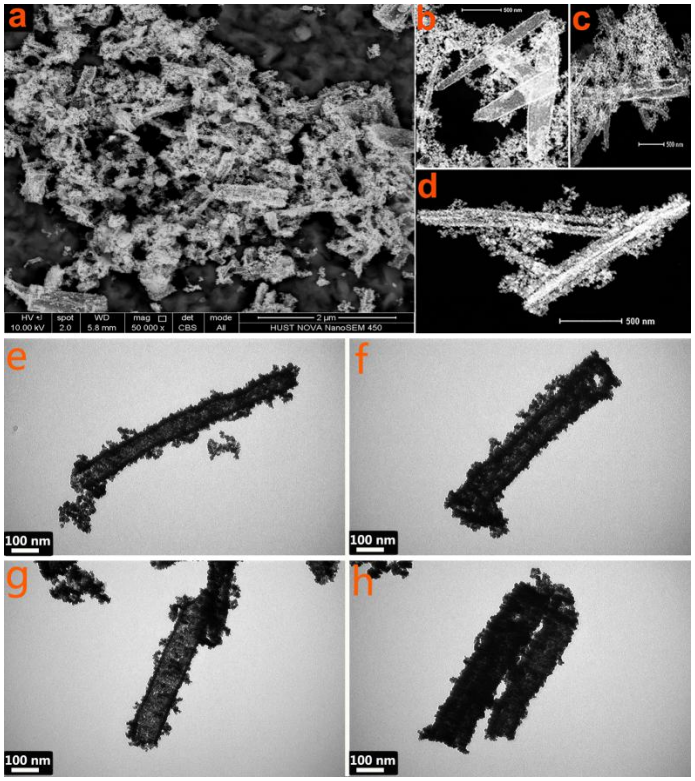

Figure S1. FESEM image of Pt -SMPB (a), and (b, c, d) HAADF-STEM images of Pt-SMPB, the supplement to the above diagram, clearly show the sub-micron porous tubes, (e, f, g, h) TEM images of the selected tube structures.

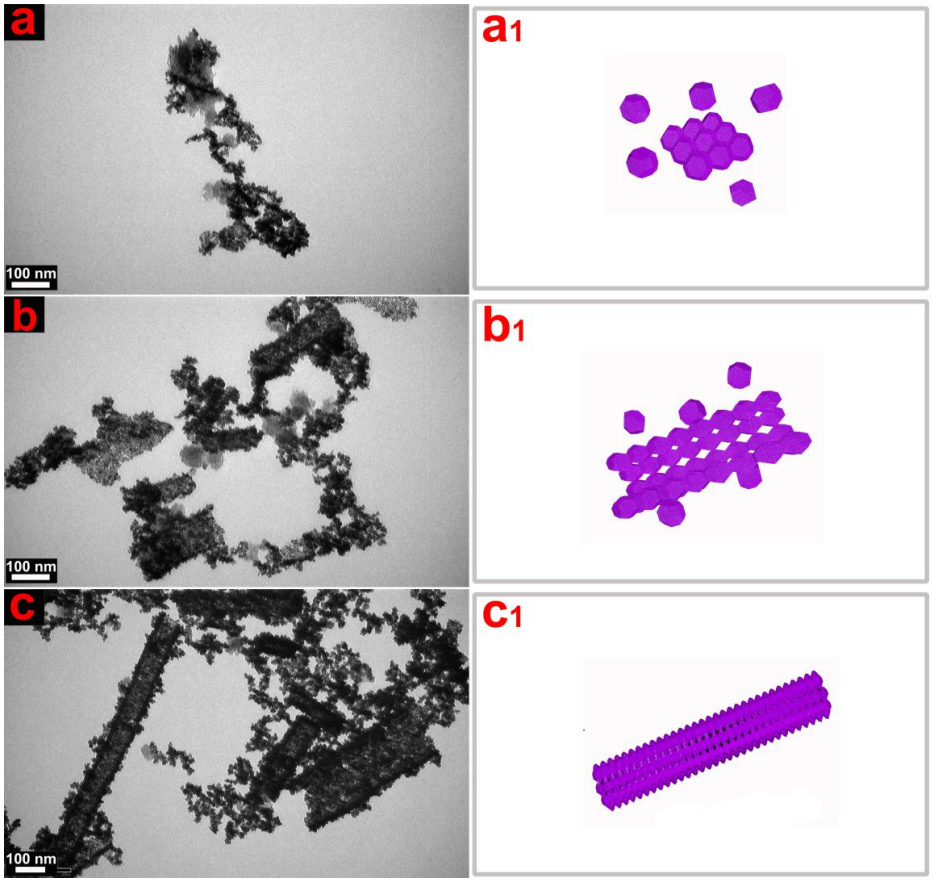

Figure S2. (a, b, c) TEM images of the samples taken during the reaction. The Pt truncated octahedral NCs assemble into two-dimensional grid and then curly become the SMPB. (a_1, b_1, c_1) The corresponding geometrical model with the (a, b, c).

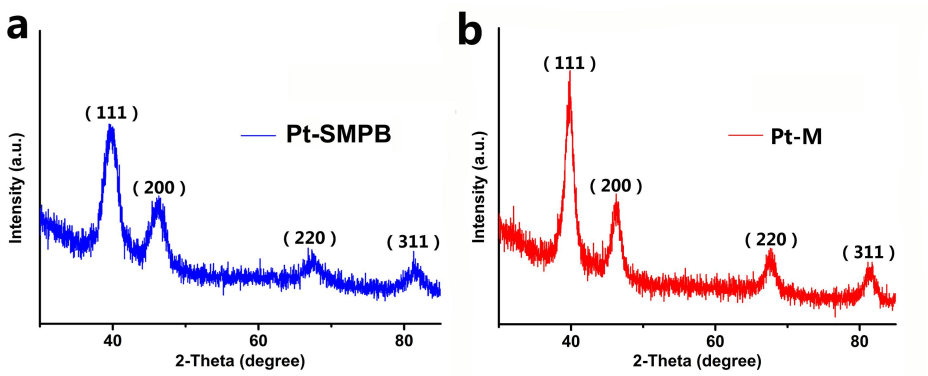

Figure S3. XRD pattern of Pt-SMPB/-M.

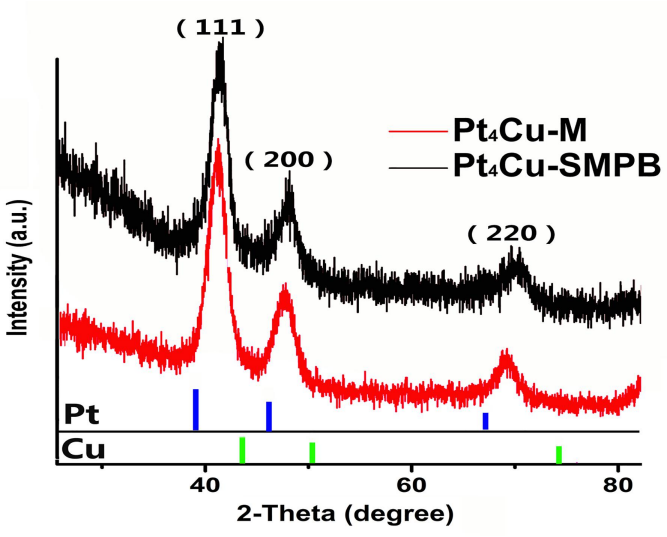

Figure S4. XRD pattern of Pt_4Cu-SMPB/-M.

Table S1. The ICP-MS for Pt/Cu composition in the Pt_4Cu-SMPB and Pt_4Cu-M.

	(63) Cu [No Gas]	(195) Pt [No Gas]
Sample	Concentration [ppm]	Concentration [ppm]
Pt_4Cu -SMPB	0.3293012	4.205273
Pt_4Cu -M	0.1723062	2.254979

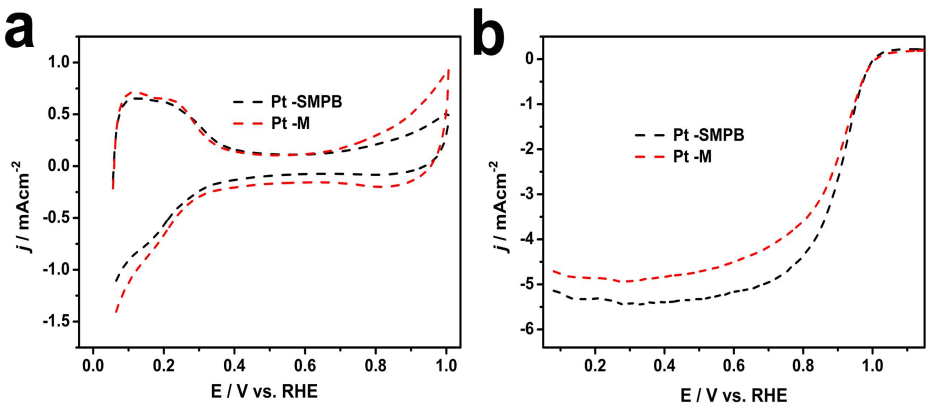

Figure S5. CVs (a) and the ORR polarization curves (b) for Pt -SMPB/ -M.

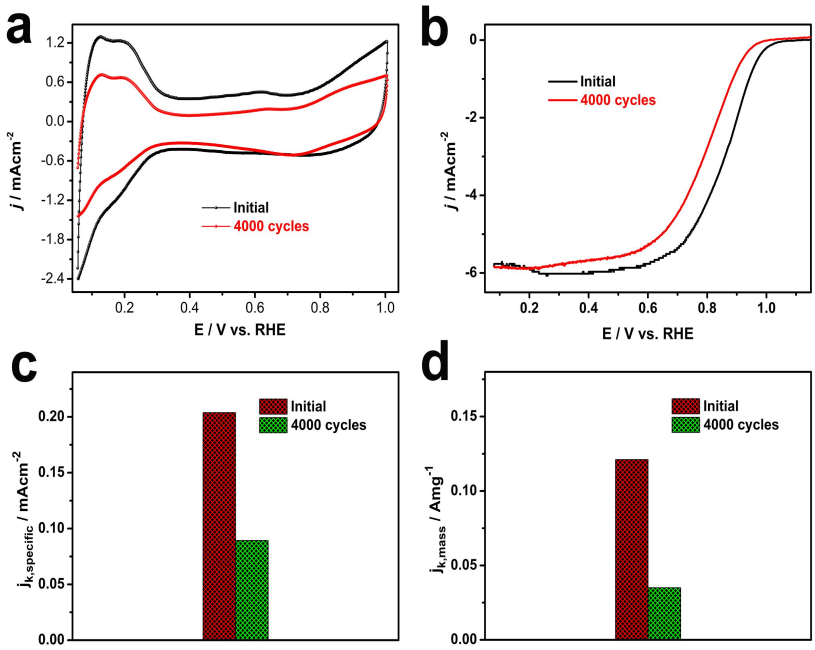

Figure S6. CVs (a) and the ORR polarization curves (b) for commercial Pt/C, before and after an accelerated durability test. $j_{k,specific}$ and $j_{k,\ mass}$ for commercial Pt/C before and after 4000 potential cycles.

Table S2. Performance of Pt_4Cu-SMPB and Pt_4Cu-M catalysts and several representative results with high performance from recent published works. (NA, not availlable).

sample	ECSA (m^2/g)	ECSA (m^2/g) after cycles	mass activity (A/mg_{Pt} at 0.90 V)	specific activity (mA/cm^2 at 0.90 V)	mass activity after cycles (A/mg_{Pt} at 0.90 V)
Pt_4Cu-SMPB (This work)	25.99	21.99	0.619	2.58	0.411
Pt_4Cu-M (This work)	21.63	18.49	0.521	2.41	0.387
$Pt_{0.3}Cu$[1]	70	NA	0.21	NA	NA
$Pt_{1.8}Cu$[1]	50	NA	0.29	NA	NA
$PtCu_3$[2]	58±6	NA	0.45±0.04	NA	NA
$PtCu$[2]	45±6	NA	0.38±0.06	0.364	NA
Pt_3Cu[2]	40±2	NA	0.23±0.02	0.531	NA
$Pt_{25}Cu_{75}$[3]	35	31.2	0.30	0.465	0.25
$Pt_{25}Cu_{75}$[3]	55	35.9	0.53	1.477	0.21
$Pt_{25}Cu_{75}$[3]	73	75.5	0.32	0.944	0.31
$PtCu_3$[4]	47±2	NA	0.41±0.09	0.873±0.167	NA
$Pt_{78}Cu_{22}$[5]	50.78	44.69	0.32	0.63	NA
$Pt_{54}Cu_{46}$[5]	41.03	NA	0.15±0.01	0.36±0.01	NA
$Pt_{37}Cu_{63}$[5]	27.71	NA	0.07±0.005	0.3±0.01	NA
PtCuNFs[6]	12.4	NA	0.211	1.71	NA
PtCu/PC-950[7]	63.2	65.3	0.043	NA	0.043
PtCu[8]	7.95	NA	5.19	0.0428	NA

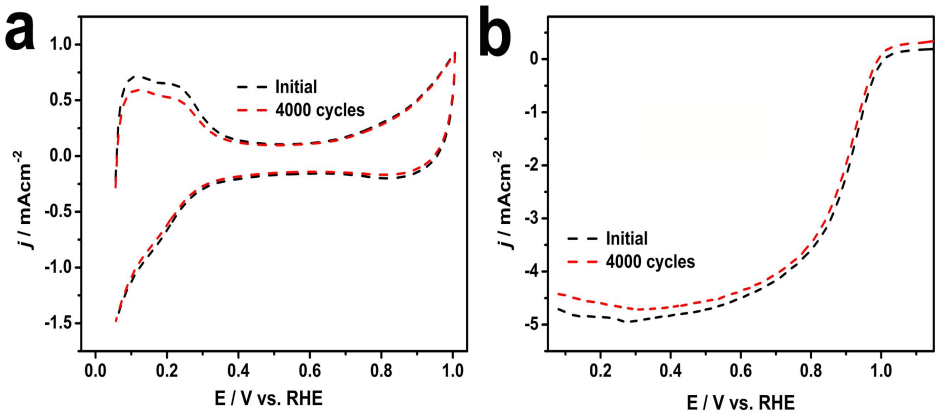

Figure S7. CVs (a) and the ORR polarization curves (b) for Pt -M, before and after an accelerated durability test.

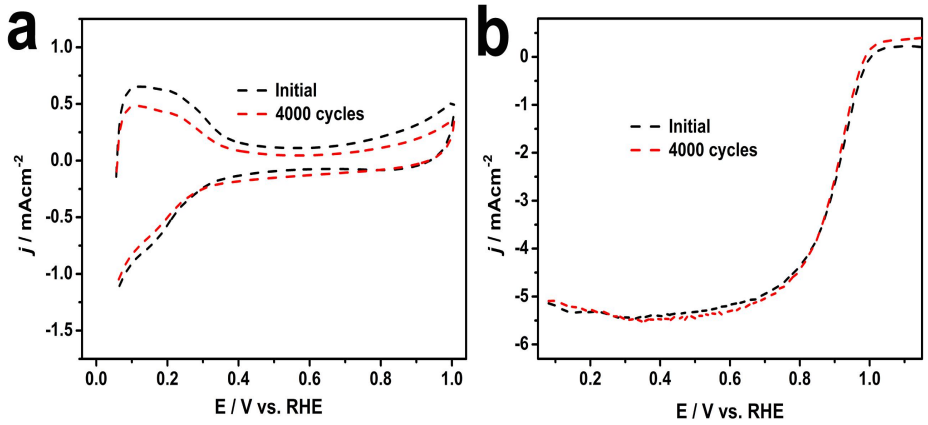

Figure S8. CVs (a) and the ORR polarization curves (b) for Pt -SMPB, before and after an accelerated durability test.

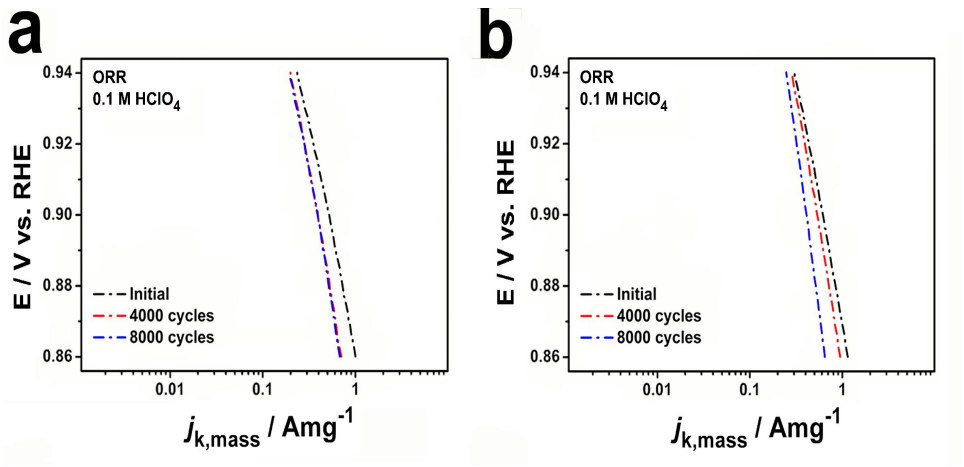

Figure S9. Mass ORR activities given as jk normalized to the loading amount of Pt of the catalysts before and after durability tests.

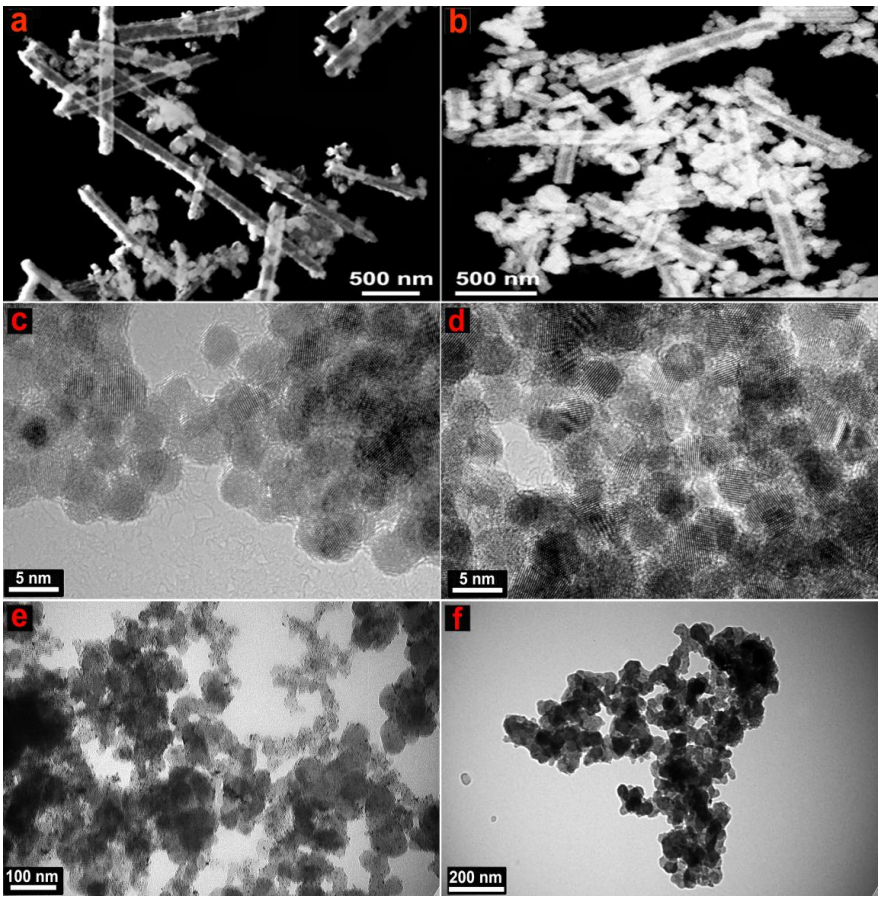

Figure S10. HAADF-STEM images of Pt_4Cu -SMPB (a) before and (b) after ADT test. (c, e) HRTEM images of Pt_4Cu -SMPB and Pt/C. (d, f) HRTEM images of Pt_4Cu -SMPB and Pt/C after cycles. The structure of sub-micron porous tubes were interrupted into several short porous tubes shown in figure S 10b, it might be caused by the strong ultrasonic cleaning the catalysts from the electrode after 8000 cycles.

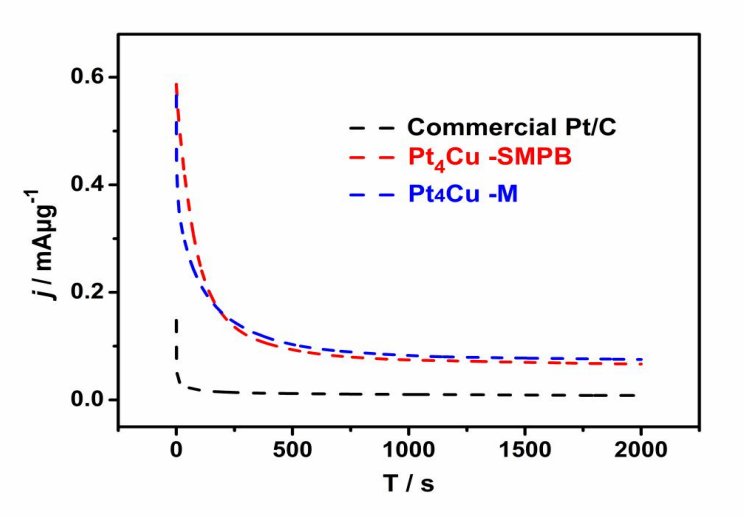

Figure S11. Current density–time curves of the Pt_4Cu -SMPB and -M and commercial Pt/C catalysts in 0.1 M $HClO_4$ + 0.2 M CH_3OH solution at 0.6 V.

Reference

1. I. Dutta, M. K. Carpenter, M. P. Balogh, J. M. Ziegelbauer, T. E. Moylan, M. H. Atwan, and N. P. Irish, *J. Phys. Chem. C*, 2010, **114**, 16309 – 16320.

2. M. Oezaslan, and P. Strasser, *J. Electrochem. Soc.*, 2012, **159**, 444 – 454.

3. K.C. Neyerlin, R. Srivastava, C. Yu, P. Strasser, *J. Power Sources*, 2009, **186**, 261 – 267.

4. M. Oezaslan, P. Strasser, *J. Power Sources*, 2011, **196**, 5240–5249.

5. S. Fu, C. Zhu, Q. Shi, H. Xia, D. Du and Y. Lin, *Nanoscale*, 2016, **8**, 5076-5081.

6. Z. Zhang, Z. Luo, B. Chen, C. Wei, J. Zhao, J. Chen, X. Zhang, Z. Lai, Z. Fan, C. Tan, M. Zhao, Q. Lu, B. Li, Y. Zong, C. Yan, G. Wang, Z. J. Xu, and H. Zhang, *Adv. Mater.*, 2016, DOI: 10.1002/adma.201603075.

7. I. Khan, Y. Qian, A. Badshah, D. Zhao, and M. Nadeem, *ACS Appl. Mater. Interfaces*, 2016, **8**, 20793–20801.

8. H. El-Deeb, M. Bron, *J. Power Sources*, 2015, **275**, 893–900.